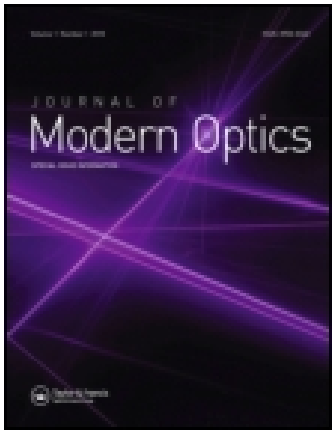

Journal of Modern Optics
Publication details, including instructions for authors and subscription information:
http://www.tandfonline.com/loi/tmop20

All-atomic generation and noise-quadrature filtering of squeezed vacuum in hot Rb vapor

Travis Horrom [a], Gleb Romanov [a], Irina Novikova [a] & Eugeniy E. Mikhailov [a]
[a] Department of Physics, The College of William and Mary, Williamsburg, VA 23187, USA
Published online: 16 Oct 2012.

Journal of Modern Optics, 2013
Vol. 60, No. 1, 43–49, http://dx.doi.org/10.1080/09500340.2012.732620

Taylor & Francis
Taylor & Francis Group

All-atomic generation and noise-quadrature filtering of squeezed vacuum in hot Rb vapor

Travis Horrom, Gleb Romanov, Irina Novikova and Eugeniy E. Mikhailov*

Department of Physics, The College of William and Mary, Williamsburg, VA 23187, USA

(*Received 10 April 2012; final version received 11 September 2012*)

With our all-atomic squeezing and filtering setup, we demonstrate control over the noise amplitudes and manipulation of the frequency-dependent squeezing angle of a squeezed vacuum quantum state by passing it through an atomic medium with electromagnetically induced transparency (EIT). We generate low sideband frequency squeezed vacuum using the polarization self-rotation effect in a hot Rb vapor cell, and direct it through a second atomic vapor subject to EIT conditions. We use the frequency-dependent absorption of the EIT window to demonstrate an example of squeeze amplitude attenuation and squeeze angle rotation of the quantum noise quadratures of the squeezed probe. These studies have implications for quantum memory and storage as well as gravitational wave interferometric detectors.

Keywords: quantum fluctuations; squeezed states; polarization self-rotation; atomic noise

1. Introduction

Squeezed light is a quantum-mechanical state of an electromagnetic field where the nonclassical photon statistics allow quadrature uncertainties to be reduced below the shot noise level, also referred to as the standard quantum limit (SQL). Since the initial observation by Slusher et al. [1], squeezed light and squeezed vacuum states have been successfully implemented to improve precise measurements in spectroscopy [2], interferometry [3–6], and magnetometry [7,8]. Squeezing has been intensely studied in relation to quantum information and quantum measurement protocols [9–12]. Studies of quantum memory realizations based on the electromagnetically induced transparency (EIT) effect [13] lead to several experiments exploring the propagation and storage of a squeezed state with EIT [14–20] in connection to quantum memory applications.

However, without tools to effectively manipulate the noise properties of squeezed states, their applications are somewhat limited. In particular, enhancing the sensitivity of gravitational wave detectors based on interferometers (such as LIGO) with squeezing requires frequency-dependent squeezing angles, or at least degrees of squeezing which can combat the greater effects of radiation pressure noise at lower detection frequencies [5]. Such a manipulation of squeezing is possible with an optical cavity [21], but it requires a narrow cavity linewidth below 1 kHz, set by LIGO internal cavities. Such a high finesse cavity would be large and bulky (on the order of 10 m or larger) even with ultra-high reflecting mirrors.

It was suggested by Mikhailov et al. [22] that narrow optical transmission resonances arising from coherent interaction with atoms (known as electromagnetically induced transparency (EIT) resonances) could be used to create frequency-dependent filters for the quadrature noise amplitude and angle in squeezed light states to be used in gravitational wave detection. Examples of the amplitude filtering effect of squeezed vacuum with EIT have been observed [14–20]. However, to the best of our knowledge the frequency-dependent squeezing angle manipulation has not yet been demonstrated.

In the above experiments demonstrating quantum noise filtering and atomic memory, the squeezed vacuum probes were generated using frequency doubling nonlinear crystals used in optical parametric oscillators (OPOs). This method has been shown to generate more than 11 dB noise reduction [23] at 1064 nm, however such high squeezing has not been shown to extend down to the lower wavelengths required for EIT experiments due to increased losses in nonlinear crystals. As a result, groups using nonlinear crystal based squeezers for EIT experiments with Rb atoms at 795 nm typically use around 3 dB noise suppressed squeezed states [14–19]. Crystal squeezing

*Corresponding author. Email: eemikh@wm.edu

also suffers from a high experimental complexity and high laser power requirements.

In this paper, we demonstrate the EIT noise amplitude filtering and *frequency-dependent* squeezing angle manipulation in an experimental setup using only atomic vapors, for both squeezing generation and manipulation. Our squeezer utilizes the polarization self-rotation effect in hot Rb vapor [24,25]. This squeezing method offers upwards of 3 dB noise suppression [26] at low sideband frequencies (200 Hz–2 MHz) [8], with an economical all-atomic experimental design, using low laser powers and neither nonlinear crystals nor optical cavities. We also observe that excess noise may couple into the system due to the back action of light noise onto the atoms. Understanding the interaction of squeezed vacuum with EIT-like media is important not only in filtering applications, but also for vapor quantum memory protocols.

2. Theory

Utilizing the two-photon formalism developed by Caves and Schumaker [27,28], we use the following expressions for amplitude (X_+) and phase (X_-) quadrature operators

$$X_+ = \frac{a(\Omega) + a^\dagger(-\Omega)}{2^{1/2}}, \tag{1}$$

$$X_- = \frac{a(\Omega) - a^\dagger(-\Omega)}{\mathrm{i}\,2^{1/2}}, \tag{2}$$

where a and $a^\dagger$ are operators of annihilation and creation of a photon at sideband frequency Ω with respect to the light carrier frequency. The quantum noise power of the corresponding quadrature is equal to the variance of the quadrature ($V_\pm = \langle X_\pm^2 \rangle - \langle X_\pm \rangle^2$). In this normalization, coherent unsqueezed states have $V_\pm = 1$. This corresponds to the case of shot noise, or the standard quantum limit (SQL). A coherent squeezed state then has one quadrature variance smaller than 1 while the product $V_+ \times V_- = 1$. Such a squeezed coherent state however is very hard to obtain in practice, and usually in the lab, one measures squeezed states where $V_+ \times V_- \geq 1$. This is true in our experiment where quadrature noise powers are about -2 dB for the minimum (squeezed) noise quadrature and 8 dB for maximum (antisqueezed) noise quadrature (see for example Figure 2, discussed in Section 3).

When a quantum light state interacts with a medium which has the complex field transmission coefficient

$$\mathcal{T}(\pm\Omega) = T_\pm \exp(\mathrm{i}\Theta_\pm), \tag{3}$$

due to the changes to light transmission and phase, the noise levels are altered according to the following equation derived in [22]

$$\begin{pmatrix} V_{+_{\mathrm{out}}} \\ V_{-_{\mathrm{out}}} \end{pmatrix} = \begin{pmatrix} A_+^2 & A_-^2 \\ A_-^2 & A_+^2 \end{pmatrix} \begin{pmatrix} V_{+_{in}} \\ V_{-_{in}} \end{pmatrix} + \begin{pmatrix} 1 - (A_+^2 + A_-^2) \\ 1 - (A_+^2 + A_-^2) \end{pmatrix}. \tag{4}$$

Here, $A_\pm \equiv \frac{1}{2}(T_+ \pm T_-)$. The first term of the above equation corresponds to attenuation/absorption of the propagating field, and the second takes into account the vacuum state which couples in and replaces the absorbed input field. Due to accumulated phase shifts of the positive and negative sidebands, the squeezed state might experience a rotation of the squeezing angle by

$$\phi = \frac{1}{2}(\Theta_+ + \Theta_-). \tag{5}$$

For a symmetrical resonance lineshape, the Kramers–Kronig relationships dictate that $\Theta_+ = -\Theta_-$, thus ϕ is zero and no rotation occurs.

Given the input noise for the squeezed and antisqueezed quadratures of a signal, and knowing the light transmission lineshape through EIT, we can use these equations to predict the output quadrature noise levels.

3. Experimental setup

The arrangement of our experiment is shown in Figure 1. Its three main components are the squeezer, where squeezed vacuum is generated, the EIT cell, where filtering occurs, and the balanced homodyne detector, which boosts the optical quantum noise above the electronic dark noise allowing it to be measured. Both the squeezer and EIT filter contain a Pyrex cell (length 75 mm) containing isotopically-enriched ^{87}Rb vapor surrounded by three layers of μ-metal magnetic shielding. The squeezing cell contains pure ^{87}Rb vapor while the EIT cell contains an additional 2.5 T neon buffer gas.

Our method for generating squeezed vacuum relies on the polarization self-rotation effect (PSR) suggested in [24]. This technique has been successfully demonstrated by several groups to date [8,25,26,29–34]. When a strong linearly polarized pump beam interacts resonantly with an atomic medium, quantum fluctuations in the orthogonal vacuum field cause slight ellipticities which lead to polarization rotations via PSR. While the strong linear field is little affected, the vacuum state becomes quadrature squeezed.

Our squeezer apparatus is the same as in our previous experiments [8,34] We start with the output of

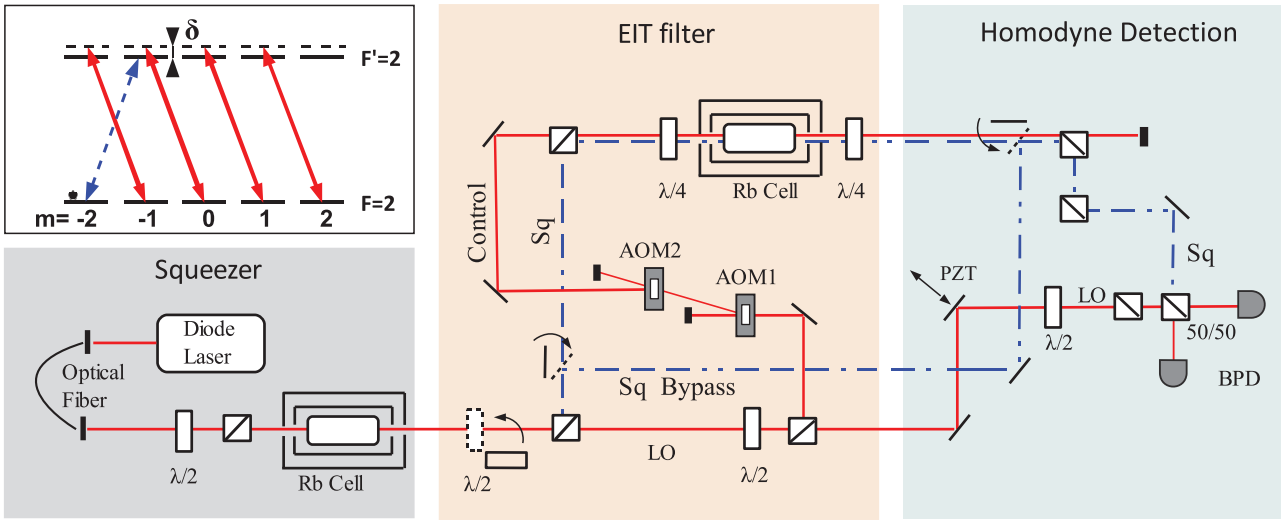

Figure 1. Experimental setup: λ/2 – half-wave plate, λ/4 – quarter-wave plate, Sq – squeezed vacuum, LO – local oscillator, AOM – acousto-optical modulator, BPD – balanced photodetector. The insert shows relevant ^{87}Rb sublevels and optical fields. The weak probe field is depicted with dashed lines, the control with solid. δ is the two-photon detuning. (The color version of this figure is included in the online version of the journal.)

a DL100 Toptica external cavity semiconductor laser tuned to the D_1 line $F_g = 2 \rightarrow F_e = 2$ transition of ^{87}Rb. A single-mode polarization-maintaining fiber outputs a clean symmetric Gaussian mode which passes through a high quality Glan-laser polarizer to ensure linear polarization of the beam. The beam then focuses to a 1001μm diameter beam waist inside the first ^{87}Rb vapor cell which acts as our squeezing medium.

For squeezing conditions, we choose an atomic density of 2.9×10^{11} atoms cm^{-3} (corresponding to the cell temperature of 58°C) and input laser powers ranging from 10–20 mW. We measure noise suppressions of up to 2 dB for the squeezed quadrature, as well as several dB of antisqueezing. We separate this squeezed vacuum field from the orthogonal strong pump laser field with a polarizing beamsplitter (PBS) after the squeezer. The squeezed vacuum field can be directed straight into the detection optics bypassing the EIT filter cell to check the prepared squeezed noise levels, or it can be directed through the EIT vapor cell and then to detection.

To measure the noise spectrum of the squeezed/antisqueezed vacuum state, we mix it with a local oscillator (LO) beam on a 50/50 beam splitter as part of a standard homodyne detection scheme and send the resulting signal to a spectrum analyzer (SA). The local oscillator is derived from the original squeezer pump laser field with its polarization rotated so that it matches that of the squeezed vacuum. With this experimental setup, we are able to change the path length traveled by the LO by scanning the PZT voltage to achieve different phase shifts of the LO compared with the squeezed field, and thus measure noise levels of the squeezed and antisqueezed noise quadratures. Detection requires spatial mode-matching of the squeezed beam and local oscillator on the photodiodes and we achieve a 97% interference fringe visibility. The balanced photodetection (BPD) is made up of two matched Hamamatsu photodiodes with better than 95% quantum efficiency.

In each measurement, we can compare the original squeezing levels with those modified by the EIT filter by sending the squeezed vacuum around the EIT cell instead of through it using flipper mirrors in the beam path. We can also compare the measured noise levels to the shot noise by completely blocking the squeezed vacuum state, thereby replacing it with normal vacuum which combines with the LO.

To facilitate EIT, we split the power of the strong laser field from the output of the squeezer and use part of it as the EIT control field, which overlaps and propagates almost colinearly with the squeezed vacuum through the EIT vapor cell. The quarter-wave plates on either side of the EIT cell were used to convert the polarizations of the squeezed and control light fields to circular and orthogonal polarizations while traveling through the EIT cell, and then back to linear after the cell. We then separate the squeezed beam from the control with two polarizing beam splitters (PBS) to improve polarization separation, and send it to the homodyne detector. To further reduce the EIT control field influence, we introduced a slight angular misalignment between the beams so most of

the control field misses our photodiodes and thus does not introduce large background light levels. Since the circularly polarized control field is very strong, it optically pumps most of the atoms into $F=2$ $m=-2$ ground sublevel and effectively creates a single Λ light level configuration with the squeezed field and Zeeman sublevels of the Rb (see insert in the Figure 1).

To characterize an EIT resonance we send a weak coherent probe field (instead of a squeezed field) into the EIT cell by introducing a half-wave plate after the squeezer. Since the EIT signal depends on the two-photon detuning, we sweep this detuning. This is accomplished by two different, but essentially equivalent methods. In the first case, we change the detuning of the control field with two acousto-optical modulators (AOMs), taking the negative first and first order beams, shifted by -80 MHz and $80+\delta$ MHz, respectively. The resulting control field is detuned from the probe by δ, and we have full control over the two-photon detuning. We find that due to the AC-Stark shift induced by the control field, the EIT resonance is centered around 900 kHz two-photon detuning and we were not able to fully filter the control field out, resulting in a large beat-note resonance between the LO and the control field on our noise spectrum. We removed points around this resonance from our noise spectra (see Figure 2(*b*)). For subsequent measurements, we used a second method of sweeping the EIT resonance. With the AOMs, we detuned the control field by 5 MHz and additionally introduced a magnetic field in the direction of light propagation in the EIT cell to compensate for this detuning shift. A calibrated sweep of this magnetic field corresponds to a change of the two-photon detuning. With this method, the LO-control field beat-note was placed outside of our detection band which improves the measured noise spectra by removing the large resonant peak (see spectra on Figures 3(*b*) and 4(*b*)).

During the noise EIT filter measurements, we fixed the two-photon detuning δ on top of the EIT resonance, and the overall shape of the transmission resonance vs two-photon detuning is shown with respect to this fixed detuning (see Figures 2(*a*), 3(*a*), and 4(*a*)). In this case, positive and negative frequency transmissions reflect the absolute value of $\mathcal{T}(\pm\Omega)$ in Equation (3), i.e. we directly measure $T_{\pm}$. We fit the transmission measurements to the following empirical function suggested in [35]:

$$T_{\pm} = A\frac{\Gamma^2}{\Gamma^2+(\delta_0\pm\Omega)^2} + B\frac{\Gamma(\delta_0\pm\Omega)}{\Gamma^2+(\delta_0\pm\Omega)^2} + C. \quad (6)$$

Here the first and second terms are the symmetric and anti-symmetric Lorentzian and the last constant term represents residual absorption of the light due to incoherent processes; Γ is the effective half width half maximum of the resonance; δ_0 is the shift of the EIT resonance with respect to squeezed vacuum field (essentially zero, as we keep the two-photon detuning on top of the EIT resonance); A, B, and C are the fitting parameters. Once we have the numerical expression for $T_{\pm}$, we input these transmission coefficients into Equation (4) to predict the output noise level. We did not measure the sideband phase lag $\Theta_{\pm}$ in our experiments, and so neglected the squeezing angle rotation in our calculations.

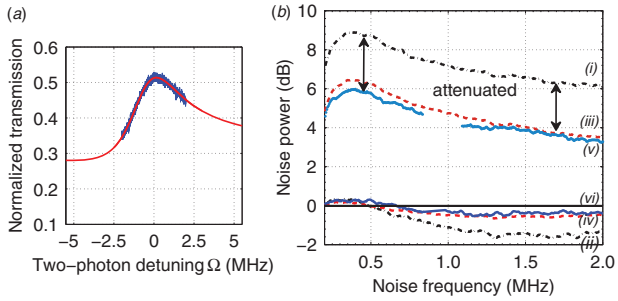

Figure 2. (*a*) EIT lineshape: solid line shows fit. Peak transmission = 52%, FWHM = 4 MHz, control power = 4.2 mW, EIT cell temperature T_{EIT}= 46°C. (*b*) Quadratures noise power spectra: (i) input max. noise, (ii) input min. noise, (iii) expected max. noise, (iv) expected min. noise, (v) measured max. noise, (vi) measured min. noise. Squeezer pump power = 21.6 mW, squeezing cell temperature $T_{\mathrm{sq}}=59$°C. We removed data points in the output noise between 0.8 and 1.1 MHz due to a large spike caused by the beatnote between the local oscillator and the control field which was detuned by 900 kHz and leaked into the detection. (The color version of this figure is included in the online version of the journal.)

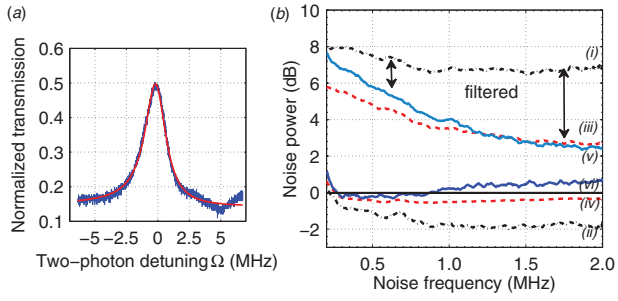

Figure 3. (*a*) EIT lineshape: solid line shows fit. Peak transmission = 50%, FWHM = 2 MHz, control power = 3.8 mW, EIT cell temperature $T_{\mathrm{EIT}}=50$°C. (*b*) Quadratures noise power spectra: (i) input max. noise, (ii) input min. noise, (iii) expected max. noise, (iv) expected min. noise, (v) measured max. noise, (vi) measured min. noise. Squeezer pump power = 13 mW, squeezing cell temperature $T_{\mathrm{sq}}=57$°C. (The color version of this figure is included in the online version of the journal.)

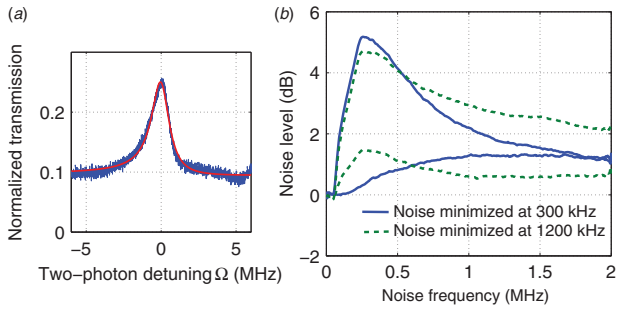

Figure 4. (*a*) EIT lineshape: solid line shows fit. Peak transmission = 25%, FWHM = 1.4 MHz, control power = 2.3 mW, EIT cell temperature $T_{\mathrm{EIT}} = 50^{\circ}\mathrm{C}$. (*b*) Quadratures noise power spectra: with noise power minimization at 300 kHz (solid-blue line) and at 1.2 MHz (dashed-green line). Squeezer pump power = 15 mW, squeezing cell temperature $T_{\mathrm{sq}} = 57^{\circ}\mathrm{C}$. (The color version of this figure is included in the online version of the journal.)

4. Experimental observations

The influence of the atomic medium on the squeezed vacuum state can be observed by comparing the input minimum and maximum noise levels to the levels measured after interaction. By attenuating the control field and thus decreasing the power broadening of the EIT resonance, or by slightly changing the control field alignment, we can narrow the EIT linewidth and change the transmission window used in the experiment. As an example of squeeze amplitude attenuation, we show two noise spectra and their associated EIT transmission curves in Figures 2 and 3. In Figure 2(*b*), we start off with a squeezed vacuum showing up to 1.5 dB noise suppression and nearly 9 dB of excess, antisqueezed noise. Any frequency dependence of the input noise levels, we attribute to laser noise which was not completely subtracted by the balanced photodiodes. This prevents us from detecting the best squeezing at the lowest noise frequencies, but this problem can be alleviated by better mode matching and alignment of the LO and the squeezed beam at the BPD, with improved beam pointing stabilization. We note that with this exact same squeezer, but using a modified squeezing detection scheme (not suitable for this experiment), we were able to generate squeezing to frequencies as low as 200 Hz [8]. For the first measurement, we make the transmission curve rather broad, with full width half maximum (FWHM) of the resonance >4 MHz (see Figure 2(*a*)), and with a fairly small contrast between the peak transmission of 52% and the background transmission of 28%. As a result, in Figure 2(*b*), the output noise levels are uniformly attenuated due to the light absorption, but there is no visible frequency-dependent filtering of the noise, since in the detection bandwidth of 2 MHz, transmission for all sidebands is almost the same. We also calculate the expected filtered noise spectra based on Equation (4) and transmission coefficients ($T_{\pm}$) extracted from the fit of the EIT transmission data (Figure 2(*a*)). We see a very good match between the theoretical prediction and the experimental data. The output noise follows along the same shape as the input noise close to the predicted noise levels, without changes in its frequency dependence. We removed data points in the output noise between 0.8 and 1.1 MHz due to a large spike caused by the beatnote between the local oscillator and the control field which was detuned by 900 kHz and leaked into the detection.

Note the difference in Figure 3. Here, as shown in Figure 3(*a*), we narrow the EIT transmission window to about 2 MHz FWHM and increase the contrast between maximum and background transmission. Now, with similar input squeezed (−2 dB) and antisqueezed (8 dB) noise levels, the output noise shows marked frequency dependence. At lower frequencies where transmission is at a maximum, the output noise levels are closer to the inputs, but at higher frequencies, we see more and more attenuation due to the light absorption at the wings of the EIT resonance. This data set shows the simple use of the EIT window as a low-pass filter. The effects of the filter are most easily observed in the antisqueezed noise quadrature due to the high amplitude, starting with 8 dB of excess noise. The squeezed quadrature also appears to follow the shape of the filter, but due to extra noise raising the noise floor, this minimum level rises above shot noise rather than settling closer to it.

We attribute this extra noise to the several potential sources. First, our numerical prediction model assumes that there is no squeezing angle rotation influencing the noise in Figures 2 and 3. This is clearly an oversimplification, because a small visible asymmetry of the EIT resonance in Figure 3 dictates, according to the Kramers–Kronig relations, that some frequency-dependent rotation should be present, which may show up as a deviation from the predicted noise levels. A second possibility is the simplicity of our model, which treats the EIT resonance as a passive absorptive filter and disregards the back action of light noise onto the atoms as well as the atomic noise contribution. This simple approach may be successful up to a point, but could lead to deviations from experiment when excess noise contributions become sizable. We note that in this experiment, the noise level resulting from blocking the squeezed probe before the EIT cell was identical to that seen when the probe was blocked after the atoms and just before detection (shot noise). This leads us to believe the atomic noise contribution is small in this case, and that most of the excess noise must then be due to back action of the light noise.

Lastly, as mentioned, any laser noise which is imperfectly balanced by the homodyne detector can raise the noise floor and add apparent frequency dependence.

Figure 4 depicts the very interesting effect of frequency-dependent squeeze angle rotation. Here, because of the asymmetry of the EIT lineshape, there is a resulting phase shift between the left and right noise sidebands leading to a rotation of the squeezing angle, which now changes with frequency. We see that the LO phase chosen for the best noise suppression at one noise frequency is not the phase giving the minimum noise level at all frequencies. This indicates that the squeezing angle has actually become frequency dependent as it rotates with frequency, requiring different phases for different noise frequencies in order to measure the maximum squeezing. Note that the noise spectrum resulting from choosing the proper phase at a lower frequency (300 kHz), looks very different from the result when the minimum noise is found by choosing the phase angle at a higher noise frequency (1200 kHz).

To the best of our knowledge this is the first reported measurement of the squeezing angle rotation done with atoms which was previously theoretically predicted in [22]. Until now the only successfully reported way to rotate the squeezing angle was with cavities [21]. Unfortunately, our data has a lot of excess noise and sub shot noise reduction did not survive after the passage through EIT.

We note that for experimental conditions corresponding to Figures 2 and 3, we did not observe such rotation. Here the squeezing angle seems to show good frequency independence.

We also demonstrate the capability to completely replace the squeezed state with an unsqueezed ordinary coherent vacuum state by changing the EIT media to a strong absorber by switching off the control field. The final plot, Figure 5, shows the output noise levels of the quantum state after the EIT filtering cell, first (*a*), while the control field is on and we sweep the local oscillator phase while recording the noise spectrum, and second (*b*), in the same situation but with the control beam completely blocked. Note that while the control beam is on, we see high phase-dependent noise levels and the squeezed vacuum is transmitted through the atoms. However, with the control off, we do not have EIT conditions and our vacuum state is absorbed by the atoms. Thus, the output noise level corresponds to shot noise, identical to the noise spectrum generated by blocking the squeezed path just before the BPD. As expected, the quantum noise is not transmitted through the atomic medium, so the noise level returns to shot noise and does not depend on the LO phase. Such a switchable filter can be of interest for quantum repeaters and quantum memory protocols.

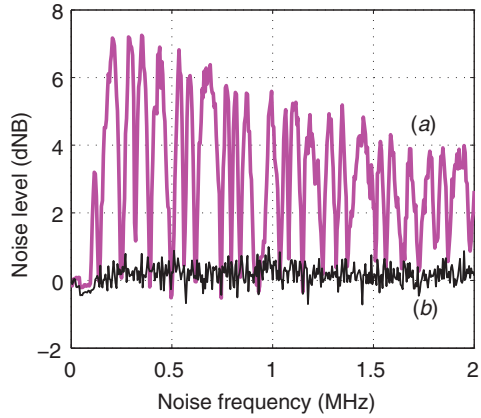

Figure 5. Noise power spectrum with control field set to 6.9 mW (*a*) and blocked (*b*). LO phase angle is continuously scanned. (The color version of this figure is included in the online version of the journal.)

5. Conclusion

We have shown an experimental demonstration of EIT used for frequency-dependent squeeze amplitude attenuation of a quantum squeezed vacuum field using only atomic vapors. In our experiment, the atoms act as a low-pass filter for squeezed and antisqueezed noise. The relative ease of controlling the transmission window in vapor cell experiments makes this method very promising for creating several different types of noise filters for squeezed vacuum. This controllable squeezed vacuum source may be easily incorporated into precision measurement experiments due to its simple, all-atomic design, and low loss.

We also observe an apparent frequency-dependent rotation of the squeezing angle as the vacuum propagates through EIT. This effect is likely due to the asymmetry of the transmission window and could also be used to create more complicated noise filters as well as to match the squeezing angle to the ponderomotive squeeze angle caused by radiation pressure in high-powered interferometers [22].

We note the less well-understood excess noise sources which couple into this experiment and degrade the noise suppression. Their contribution cannot be explained by simple treatment of the EIT resonance as a media with complex transmission coefficients. A full quantum mechanical treatment of the light–atom interaction would be needed to fully describe the extra noise sources. These dynamics of quantum noise, along with any excess noise sources, will be important to any precision measurement or quantum memory experiment which uses the interaction of squeezed light with an atomic medium.

Acknowledgement

This research was supported by NSF Grant PHY-0758010.

References

[1] Slusher, R.E.; Hollberg, L.W.; Yurke, B.; Mertz, J.C.; Valley, J.F. *Phys. Rev. Lett.* **1985,** *55,* 2409–2412.
[2] Polzik, E.S.; Carri, J.; Kimble, H.J. *Phys. Rev. Lett.* **1992,** *68,* 3020–3023.
[3] Caves, C.M. *Phys. Rev. D* **1981,** *23,* 1693–1708.
[4] Chickarmane, V.; Dhurandhar, S.V. *Phys. Rev. A* **1996,** *54,* 786–793.
[5] Kimble, H.J.; Levin, Y.; Matsko, A.B.; Thorne, K.S.; Vyatchanin, S.P. *Phys. Rev. D* **2002,** *65,* 022002.
[6] Goda, K.; Miyakawa, O.; Mikhailov, E.E.; Saraf, S.; Adhikari, R.; McKenzie, K.; Ward, R.; Vass, S.; Weinstein, A.J.; Mavalvala, N. *Nat. Phys.* **2008,** *4,* 472–476.
[7] Wolfgramm, F.; Cerè, A.; Beduini, F.A.; Predojevi ć, A.; Koschorreck, M.; Mitchell, M.W. *Phys. Rev. Lett.* **2010,** *105,* 053601.
[8] Horrom, T.; Singh, R.; Dowling, J.P.; Mikhailov, E.E. *Phys. Rev. A* **2012,** *86,* 023803.
[9] Hammerer, K.; Sørensen, A.S.; Polzik, E.S. *Rev. Mod. Phys.* **2010,** *82,* 1041–1093.
[10] Simon, C.; Afzelius, M.; Appel, J.; Boyer de la Giroday, A.; Dewhurst, S.J.; Gisin, N.; Hu, C.Y.; Jelezko, F.; Kröll, S.; Müller, J.H.; Nunn, J.; Polzik, E.S.; Rarity, J.G.; De Riedmatten, H.; Rosenfeld, W.; Shields, A.J.; Sköld, N.; Stevenson, R.M.; Thew, R.; Walmsley, I.A.; Weber, M.C.; Weinfurter, H.; Wrachtrup, J.; Young, R.J. *Eur. Phys. J. D* **2010,** *58,* 1–22.
[11] Novikova, I.; Walsworth, R.; Xiao, Y. *Laser Photonics Rev.* **2012,** *6,* 333–353. DOI: 10.1002/lpor.201100021.
[12] Walls, D.F. *Nature* **1983,** *306,* 141–146.
[13] Harris, S.E. *Phys. Today* **1997,** *50,* 36–42.
[14] Akamatsu, D.; Akiba, K.; Kozuma, M. *Phys. Rev. Lett.* **2004,** *92,* 203602.
[15] Akamatsu, D.; Yokoi, Y.; Arikawa, M.; Nagatsuka, S.; Tanimura, T.; Furusawa, A.; Kozuma, M. *Phys. Rev. Lett.* **2007,** *99,* 153602–4.
[16] Appel, J.; Figueroa, E.; Korystov, D.; Lobino, M.; Lvovsky, A.I. *Phys. Rev. Lett.* **2008,** *100,* 093602.
[17] Figueroa, E.; Lobino, M.; Korystov, D.; Appel, J.; Lvovsky, A.I. *New J. Phys.* **2009,** *11,* 013044.
[18] Honda, K.; Akamatsu, D.; Arikawa, M.; Yokoi, Y.; Akiba, K.; Nagatsuka, S.; Tanimura, T.; Furusawa, A.; Kozuma, M. *Phys. Rev. Lett.* **2008,** *100,* 093601.
[19] Arikawa, M.; Honda, K.; Akamatsu, D.; Yokoil, Y.; Akiba, K.; Nagatsuka, S.; Furusawa, A.; Kozuma, M. *Opt. Express* **2007,** *15,* 11849–11854.
[20] Arikawa, M.; Honda, K.; Akamatsu, D.; Nagatsuka, S.; Akiba, K.; Furusawa, A.; Kozuma, M. *Phys. Rev. A* **2010,** *81,* 021605.
[21] Chelkowski, S.; Vahlbruch, H.; Hage, B.; Franzen, A.; Lastzka, N.; Danzmann, K.; Schnabel, R. *Phys. Rev. A* **2005,** *71,* 013806.
[22] Mikhailov, E.E.; Goda, K.; Corbitt, T.; Mavalvala, N. *Phys. Rev. A* **2006,** *73,* 053810.
[23] Mehmet, M.; Vahlbruch, H.; Lastzka, N.; Danzmann, K.; Schnabel, R. *Phys. Rev. A* **2010,** *81,* 013814.
[24] Matsko, A.B.; Novikova, I.; Welch, G.R.; Budker, D.; Kimball, D.F.; Rochester, S.M. *Phys. Rev. A* **2002,** *66,* 043815.
[25] Mikhailov, E.E.; Novikova, I. *Opt. Lett.* **2008,** *33,* 1213–1215.
[26] Barreiro, S.; Valente, P.; Failache, H.; Lezama, A. *Phys. Rev. A* **2011,** *84,* 033851.
[27] Caves, C.M.; Schumaker, B.L. *Phys. Rev. A* **1985,** *31,* 3068–3092.
[28] Schumaker, B.L.; Caves, C.M. *Phys. Rev. A* **1985,** *31,* 3093–3111.
[29] Ries, J.; Brezger, B.; Lvovsky, A.I. *Phys. Rev. A* **2003,** *68,* 025801.
[30] Agha, I.H.; Messin, G.; Grangier, P. *Opt. Express* **2010,** *18,* 4198–4205.
[31] Mikhailov, E.E.; Lezama, A.; Noel, T.W.; Novikova, I. *J. Mod. Opt.* **2009,** *56,* 1985–1992.
[32] Horrom, T.; Balik, S.; Lezama, A.; Havey, M.D.; Mikhailov, E.E. *Phys. Rev. A* **2011,** *83,* 053850.
[33] Horrom, T.; Lezama, A.; Balik, S.; Havey, M.D.; Mikhailov, E.E. *J. Mod. Opt.* **2011,** *58,* 1936–1941.
[34] Horrom, T.; Novikova, I.; Mikhailov, E.E. *J. Phys. B: At. Mol. Opt. Phys.* **2012,** *45,* 124015.
[35] Knappe, S.; Stahler, M.; Affolderbach, C.; Taichenachev, A.; Yudin, V.; Wynands, R. *Appl. Phys. B* **2003,** *76,* 57–63.